

Kinetics and mechanism of the nitrosobenzene deoxygenation by trivalent phosphorous compounds*

V. S. Khursan, V. A. Shamukaev, E. M. Chainikova, S. L. Khursan, and R. L. Safullin*

*Institute of Organic Chemistry, Ufa Scientific Center, Russian Academy of Sciences,
71 prosp. Oktyabrya, 450054 Ufa, Bashkortostan, Russian Federation.*

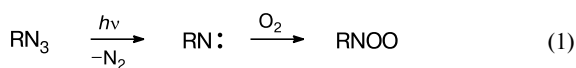
Fax: +7 (347) 235 6066. E-mail: kinetic@anrb.ru

The reaction of aryl nitroso compounds with organic phosphines and phosphites in aerated media is a convenient non-photolytic procedure to generate aromatic nitroso oxides. The reaction rate constants and activation parameters of the key (for the proposed method of nitroso oxide generation) reaction of nitrosobenzene with triphenyl phosphite or *para*-substituted phosphines (4-RC₆H₄)₃P (R = MeO, Me, H, F), as well as that of *para*-methoxynitrosobenzene with triphenylphosphine in acetonitrile were determined by kinetic spectrophotometry and chemiluminescence. A significant transfer of the electron density to the nitroso compound occurs in the transition state of the reaction as was revealed using the Hammett correlation analysis and DFT calculations in the M06L/6-311+G(d,p) approximation. The introduction of the electron-donor substituent MeO into the *para*-position of PhNO decreases the reactivity of the nitroso compound by two orders of magnitude. The reactivity of triphenyl phosphite in the oxygen atom transfer reaction is lower by two orders of magnitude compared to that of triphenylphosphine. In the case of the reactions of PhNO with phosphines, the apparent rate constant depends on the oxygen content in the reaction medium.

Key words: nitrosobenzenes, triphenyl phosphite, triphenylphosphines, kinetic spectrophotometry, chemiluminescence, DFT calculations, mechanism, reaction kinetics.

Investigation of chemical properties of active intermediates in chemical reactions is one of the most intensely studied directions of modern chemistry. Nitroso oxides RNOO play an important role in the oxidation and photooxidation of a series of nitrogen-containing organic compounds. The chemical properties and reactivity of these compounds are being actively studied in our research group^{1–11} and all over the world.^{12–19} The most frequently used method for nitroso oxide generation is the photooxidation of the corresponding azides that proceeds through the nitrene intermediates (Scheme 1).

Scheme 1



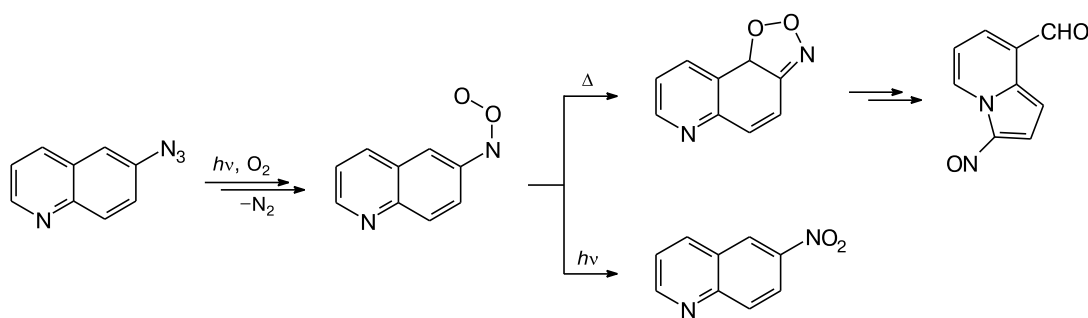
In particular, this method generates aromatic nitroso oxides ArNOO both under the conditions of matrix isolation^{13–16} and in solution.^{13,14,17–19} However, this method has an obvious drawback: under the stationary photolysis conditions, both aromatic nitroso oxides that absorb

in the visible spectral range^{4,13,14} and the products of their transformation can undergo photolytic transformations, which impedes the interpretation of the experimental results. The minor product of 6-azidoquinoline photooxidation is 6-nitroquinoline formed due to the photoisomerization of the corresponding nitroso oxide.^{20,21} The product of thermal consumption of 6-nitroquinoline is dioxazole decomposing according to Scheme 2.

Therefore, it is necessary to develop a procedure for the efficient generation of aromatic nitroso oxides under the conditions excluding the photolysis of the reaction system. It is known²² that the thermal deoxygenation of nitrobenzenes by trivalent phosphorus compounds (phosphines and phosphites) is a convenient method for generation of the corresponding nitrenes (Scheme 3). If this reaction occurs under an oxygen atmosphere, it can serve as a source of nitroso oxides formed by the further oxidation of nitrenes. The reduction of nitrosobenzene and *para*-methoxynitrosobenzene in acetonitrile at room temperature was studied²³ using triphenylphosphine as an example. Based on an analysis of the reaction products, the authors suggested the chain character of the process and partial regeneration of nitrosobenzene upon the reaction of *trans*-nitroso oxide with triphenylphosphine. However, the kinetic regularities of reaction (2) were not studied earlier. As far as we know, there is only one work²⁴ pre-

* Dedicated to Academician of the Russian Academy of Sciences M. P. Egorov on the occasion of his 60th birthday.

Scheme 2



senting the kinetic data on the reaction of 2-nitrosobiphenyl with triethyl phosphite in triethyl phosphate taken as a solvent, where it was found that $\log A = 6.9$ ($L \text{ mol}^{-1} \text{ s}^{-1}$), $E_a = 48 \text{ kJ mol}^{-1}$. Note that the rate constant of this reaction characterizes the efficiency of nitrene generation (and, therefore, nitroso oxides) and is the key characteristic of the proposed non-photocatalytic method of ArNOO generation.

Scheme 3



This work is devoted to studying the kinetics of the reactions of nitrosobenzene with a series of *para*-substituted phosphines. The kinetic data for the reactions of *para*-methoxynitrosobenzene with triphenylphosphine and of nitrosobenzene with triphenyl phosphite are given for a comparison. The kinetics of the process was studied by spectrophotometry from the absorbance decay of the nitroso compound and by chemiluminescence (CL), which is observed in the reactions of ArNO with aromatic phosphines.²⁵

Experimental

Acetonitrile (special purity grade (0)) for HPLC (Kriokhrom) was used without preliminary purification. Nitrosobenzene and 4-methoxynitrosobenzene were synthesized according to known procedures.^{26,27} Phosphines $(4\text{-RC}_6\text{H}_4)_3\text{P}$ (R = MeO, Me, H, F) were recrystallized from ethanol. Triphenyl phosphite $(\text{PhO})_3\text{P}$ was synthesized by the reaction of PCl_3 with phenol.²⁸

Method of kinetic spectrophotometry (KSP). The studies were carried out on a Shimadzu UV-365 spectrometer. A temperature-maintained cell with an optical path length of 1 cm served as a reactor. A solution of phosphine (phosphite) in acetonitrile, whose concentration was varied in the range $(0.5\text{--}4) \cdot 10^{-3} \text{ mol L}^{-1}$, was preliminarily flushed with argon or oxygen and nitrosobenzene $(2 \cdot 10^{-4} \text{ mol L}^{-1})$ was rapidly added. The absorbance decay was detected in time at the long-wavelength absorption maximum ($\lambda_{\text{max}} = 755 \text{ nm}$), which corresponds

to the forbidden transition $n \rightarrow \pi^*$. Each experiment was carried out at least three times. Experiments with 4-methoxynitrosobenzene were monitored at the wavelength corresponding to the absorption band maximum $\lambda_{\text{max}} = 730 \text{ nm}$. This wavelength was chosen because the used aromatic phosphorus(III) compounds, intermediates, and reaction products are transparent in this wave range. The digitized kinetic curves at the reaction depth at least 90% were processed in the framework of the first-order kinetic equation, and the effective rate constant of nitrosobenzene consumption (k_{eff}) was determined. This value depended linearly on the initial concentration of the phosphorus(III) compound, and the angular coefficient of the dependence $k_{\text{eff}}/[\text{R}_3\text{P}]_0$ was numerically equal to the rate constant of reaction (2). The activation parameters of reaction (2) were determined in the temperature range from 281 to 321 K using the above described procedure of monitoring the nitrosobenzene concentration under the conditions of a significant (as a rule, 20-fold) excess of R_3P .

Chemiluminescence method. The reactions of nitrosobenzene with triarylphosphines were carried out in a glass reactor equipped with a stirrer, a bubbler (experiment was made in air and under argon), and an injector using acetonitrile as a solvent with temperature varying from 293 to 323 K. A solution (1.5 mL) of nitrosobenzene was injected into a solution (13.5 mL) of triphenylphosphine with a known concentration and the change in the CL intensity in time was detected. Under the experimental conditions, the time of mixing reactants did not exceed 1 s. A FEU-119 photoelectron multiplier, whose spectral sensitivity range varies from 330 to 650 nm, was used as a detector.

DFT calculations. Theoretical simulation of the reaction of nitrosobenzene with R_3P was performed using the Gaussian-09, Revision C1 program package.²⁹ The ChemCraft program³⁰ was used for the visualization of the obtained results. The DFT methods B3LYP,^{31,32} CAM-B3LYP,³³ TPSSSTPSS and TPSSh,³⁴ LC-wPBE,³⁵ M06,³⁶ and M06L³⁷ in combination with the 6-311+G(d,p) basis set^{38,39} were used to optimize the geometric parameters and to calculate the vibrational spectra. The correspondence of the determined structures to minima on the potential energy surface was established by the absence of negative elements in the diagonalized Hesse matrix. The influence of the solvent was taken into account using the polarizable continuum model IEFPCM.⁴⁰ Wave functions of transition states were analyzed by the NBO⁴¹ and AIM⁴² methods. All calculations were performed at the Supercomputer Cluster of the Center of Collective Use of the Institute of Organic Chemistry (Ufa Scientific Center, Russian Academy of Sciences).

Results and Discussion

Reaction of nitrosobenzene with triphenyl phosphite.

Kinetic spectrophotometry is a convenient method to study the kinetics of the reactions of phosphites with substituted nitrosobenzenes, since the absorption of one of the components (ArNO) can be separated from the absorption of other compounds of the reacting system. For example, it is known that triphenyl phosphite and triphenyl phosphate absorb in the UV spectral range with the band maxima at 265 nm ($\epsilon = 1750 \text{ L mol}^{-1} \text{ cm}^{-1}$) and 262 nm ($\epsilon = 810 \text{ L mol}^{-1} \text{ cm}^{-1}$), respectively.⁴³ Nitrosobenzene exhibits an intense absorption at 250 nm ($\epsilon = 19\,000 \text{ L mol}^{-1} \text{ cm}^{-1}$)⁴³ and a weak band in the far visible spectral range corresponding to the forbidden transition $n \rightarrow \pi^*$. According to our data, the long-wavelength absorption maxima of nitrobenzene and *para*-methoxynitrosobenzene in acetonitrile lie at 755 nm ($\epsilon = 43 \text{ L mol}^{-1} \text{ cm}^{-1}$) and 730 nm ($\epsilon = 52 \text{ L mol}^{-1} \text{ cm}^{-1}$), respectively.

It turned out that the reaction of nitrosobenzenes with phosphites occurs with fairly low rates, which makes this system to be less promising from the viewpoint of efficient generation of considerable amounts of nitroso oxide. Therefore, in this work, we restricted the study by the interaction of triphenyl phosphite (PhO)₃P with nitrosobenzene PhNO. In this case, the equation of reaction (2) takes the form shown in Scheme 4.

Scheme 4



The kinetics of reaction (2a) was studied at the absorption maximum of the nitroso compound under the conditions of the pseudo-first order from its concentration, *i.e.*, under the conditions that $[(\text{PhO})_3\text{P}]_0 = 5 \cdot 10^{-2} \text{ mol L}^{-1} \gg \gg [\text{PhNO}]_0 = 2 \cdot 10^{-3} \text{ mol L}^{-1}$. Acetonitrile was used as a solvent and the reaction was carried out in aerated solutions in the temperature range from 293 to 333 K. The further temperature rise is impossible because of a substantial evaporation of the solvent. According to the law of active masses, the change in the PhNO concentration is the following:

$$-d[\text{PhNO}]/dt = k_{2a}[\text{PhNO}](\text{PhO})_3\text{P}. \quad (I)$$

Taking into account that a 25-fold excess of triphenyl phosphite is used in the reaction, it can be considered that its concentration remains almost unchanged in the reaction course and this kinetic equation can be written in the integral form

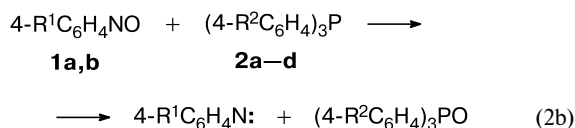
$$[\text{PhNO}] = [\text{PhNO}]_0 \cdot \exp(-k_{\text{eff}}t), \quad (II)$$

where $k_{\text{eff}} = k_{2a}[(\text{PhO})_3\text{P}]_0$.

Equation (II) with a high correlation coefficient is fulfilled in the whole range of times and temperatures, which makes it possible to calculate the rate constant of reaction (2a), k_{2a} , we are interested in (Table 1). The data of Table 1 were processed in the coordinates of the Arrhenius equation, and the activation parameters of reaction (2a) were determined (Table 2). The obtained results with allowance for differences in the objects of the study and the solvent are well consistent with the published data²⁴: the pre-exponential factors coincide within the experimental error and the activation energy of the reaction of 2-nitrosobiphenyl with triethyl phosphite in triethyl phosphate is lower by 12 kJ mol⁻¹ than that found by us. The low activation energy provides the rate constant determined for trialkyl phosphite higher by approximately an order of magnitude, and the triphenyl phosphite used is less active in the deoxygenated of nitrosobenzenes.

Reaction of nitrosobenzenes with phosphines. To continue the investigation of the kinetics of ArNO deoxygenation by organic phosphorus(III) compounds, we studied the kinetic regularities of the reactions of nitrosobenzene (**1a**) and *para*-methoxynitrosobenzene (**1b**) with a series of substituted aromatic phosphines **2a–d** in acetonitrile. The primary products of these reactions are *para*-substituted phenylnitrenes and *para*-substituted aromatic phosphine oxides (Scheme 5).

Scheme 5



1: R¹ = H (**a**), MeO (**b**); **2:** R² = H (**a**), MeO(**b**), Me (**c**), F (**d**)

On the whole, the procedure of studying the kinetics of reaction (2b) is similar to that described above. Since phosphines are more reactive than triphenyl phosphite, the initial concentration of the nitroso compound was decreased by approximately an order of magnitude ($[\text{PhNO}]_0 \approx 2 \cdot 10^{-4} \text{ mol L}^{-1}$) to attain reasonable reaction times. As a result, the absorbance of ArNO did not exceed 0.01 in the course of the reaction. Nevertheless, computer simulation of the digitized signal made it possible to obtain rather reliable and reproducible data. Figure 1 shows the typical kinetic curves of absorbance decay. It is seen that *A* decreases to zero, *i.e.*, the reaction products do not absorb at the monitoring wavelength. In fact, according to published data,⁴³ phosphine oxide Ph₃PO has an absorption band in the UV range with a maximum at 265 nm ($\epsilon = 1550 \text{ L mol}^{-1} \text{ cm}^{-1}$). It was found that k_{eff} calculated by kinetic data processing increased linearly with an increase in the initial phosphine concentration (Fig. 2). The rate constant of the reaction of **1a** with phosphines **2a–d** was determined from the slope ratio of this dependence (see Table 1).

Table 1. Rate constants of the reactions of nitrosobenzene (**1a**) with organic phosphorus(III) compounds in acetonitrile

R ₃ P	Atmosphere	T/K	[R ₃ P] ₀ /mol L ⁻¹	k ₂ ^a /L mol ⁻¹ s ⁻¹	Method
(PhO) ₃ P	Air	293	5 · 10 ⁻²	6.2 · 10 ⁻⁴	KSP
	Air	303	5 · 10 ⁻²	2.3 · 10 ⁻³	KSP
	Air	313	5 · 10 ⁻²	3.1 · 10 ⁻³	KSP
	Air	323	5 · 10 ⁻²	5.5 · 10 ⁻³	KSP
	Air	333	5 · 10 ⁻²	1.6 · 10 ⁻²	KSP
Ph ₃ P	Air	293	(0.5–4) · 10 ⁻³	3.2	KSP
	Air	293	1 · 10 ⁻²	3.1	CL
	Air	303	1 · 10 ⁻²	4.4	CL
	Air	313	1 · 10 ⁻²	6.5	CL
	Air	323	1 · 10 ⁻²	8.8	CL
	Argon	293	(0.5–3) · 10 ⁻³	5.6	KSP
	Argon ^b	293	(0.5–3) · 10 ⁻³	7.2	KSP
	Argon	281	1 · 10 ⁻³	4.6	KSP
	Argon	291	1 · 10 ⁻³	6.1	KSP
	Argon	301	1 · 10 ⁻³	11	KSP
	Argon	321	1 · 10 ⁻³	20	KSP
Ph ₃ P ^c	Air	293	(2–8) · 10 ⁻³	4.4 · 10 ⁻²	KSP
(4-MeOC ₆ H ₄) ₃ P	Air	293	(0.5–2) · 10 ⁻³	19	KSP
	Air	293	5 · 10 ⁻³	15	CL
	Air	303	5 · 10 ⁻³	18	CL
	Air	313	5 · 10 ⁻³	21	CL
	Air	323	5 · 10 ⁻³	23	CL
	Argon	293	(0.5–2) · 10 ⁻³	~30	KSP
(4-MeOC ₆ H ₄) ₃ P ^c	Air	293	(2–10) · 10 ⁻³	0.23	KSP
(4-MeC ₆ H ₄) ₃ P	Air	293	(1–4) · 10 ⁻³	4.7	KSP
	Air	293	5 · 10 ⁻³	13	CL
	Air	303	5 · 10 ⁻³	17	CL
	Air	313	5 · 10 ⁻³	19	CL
	Air	323	5 · 10 ⁻³	21	CL
	Argon	293	(0.5–1.5) · 10 ⁻³	22	KSP
	Argon	281	1 · 10 ⁻³	18	KSP
	Argon	291	1 · 10 ⁻³	21	KSP
	Argon	301	1 · 10 ⁻³	25	KSP
	Argon	311	1 · 10 ⁻³	30	KSP
(4-MeC ₆ H ₄) ₃ P ^c	Air	293	(2–6) · 10 ⁻³	0.12	KSP
(4-FC ₆ H ₄) ₃ P	Air	293	(0.5–4) · 10 ⁻³	2.8	KSP
	Air	293	5 · 10 ⁻³	2.8	CL
	Air	303	5 · 10 ⁻³	5.0	CL
	Air	313	5 · 10 ⁻³	6.6	CL
	Air	323	5 · 10 ⁻³	9.5	CL
	Argon	293	(0.5–2) · 10 ⁻³	4.3	KSP
	Argon ^b	293	(0.5–2) · 10 ⁻³	4.7	KSP
	Argon	281	1.5 · 10 ⁻³	1.8	KSP
	Argon	291	1.5 · 10 ⁻³	4.3	KSP
	Argon	301	1.5 · 10 ⁻³	4.9	KSP
	Argon	311	1.5 · 10 ⁻³	8.9	KSP
	Argon	321	1.5 · 10 ⁻³	11	KSP
	(4-FC ₆ H ₄) ₃ P ^c	Air	293	(4–8) · 10 ⁻³	1.4 · 10 ⁻²

^a The inaccuracy of the kinetic curve approximations, as a rule, was 1–2% and did not exceed 10%. In all cases, the initial concentration of the phosphorus(III) compound exceeded the initial nitrobenzene concentration by at least an order of magnitude.

^b Argon was specially purified from oxygen.

^c The reaction with *para*-methoxynitrosobenzene (**1b**).

Table 2. Arrhenius parameters of the rate constant according to the experimental data and the DFT calculations of the transition state for the reactions of nitrosobenzene with the organic phosphorus(III) compounds

Reaction	KSP		CL		M06L/6-311+G(d,p)			
	logA (logk)	E_a /kJ mol ⁻¹	logA	E_a /kJ mol ⁻¹	ΔH^\ddagger (gas phase)	$\Delta\Delta G_{\text{solv}}$	ΔH^\ddagger (MeCN)	$-\Delta S^\ddagger$ /kJ mol ⁻¹ K ⁻¹
					kJ mol ⁻¹			
PhNO + 2b	(-1.28, 293K)	—	3.1±0.1	11±1	31.7	-19.7	12.1	188
PhNO + 2c	3.6±0.1	13±1	3.2±0.2	12±1	33.6	-17.0	16.6	200
PhNO + 2a	5.9±0.4	29±3	5.4±0.1	28±1	39.4	-14.7	24.7	188
PhNO + 2d	6.5±0.7	33±1	6.0±0.5	31±3	40.4	-14.4	26.1	196
4-MeOC ₆ H ₄ NO + 2a	(-1.36, 293K)	—	5.6±0.2	40±1	55.5	-8.6	46.8	181
PhNO + (PhO) ₃ P	7.5±1.2	60±7	—	—	69.5	6.9	76.4	219

Notes. A (L mol⁻¹ s⁻¹) is the pre-exponential factor, E_a is the activation energy, ΔH^\ddagger is the activation enthalpy, $\Delta\Delta G_{\text{solv}}$ is the solvation energy, and ΔS^\ddagger is the activation entropy.

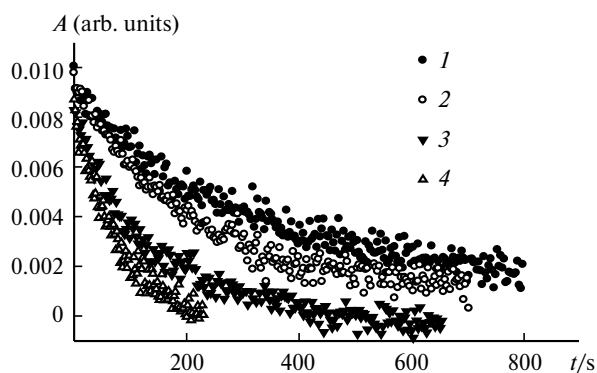


Fig. 1. Typical kinetic curves of the absorbance decay in the reactions of nitrosobenzenes with aromatic phosphines for the reaction of PPh₃ (**2a**) with nitrosobenzene (**1a**) at the initial concentrations of **2a** equal to $5 \cdot 10^{-4}$ (**1**), $1 \cdot 10^{-3}$ (**2**), $2 \cdot 10^{-3}$ (**3**), and $4 \cdot 10^{-3}$ mol L⁻¹ (**4**). Reaction conditions: initial nitrosobenzene concentration $[1a]_0 = 2 \cdot 10^{-4}$ mol L⁻¹, MeCN, 293 K, oxygen bubbling.

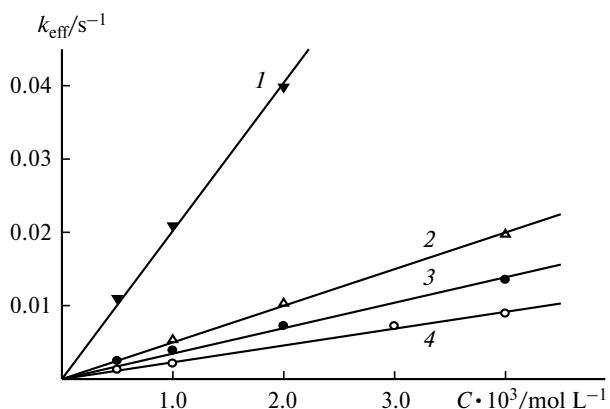
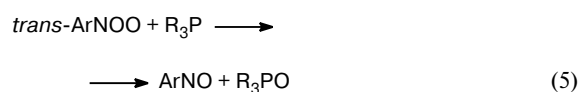
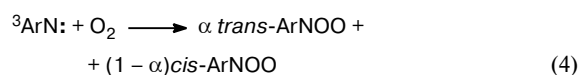
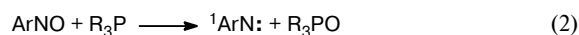


Fig. 2. Effective rate constants of the reactions of **1a** with phosphines **2b** (**1**), **2c** (**2**), **2a** (**3**), and **2d** (**4**) vs concentration of introduced phosphine (C). Reaction conditions: MeCN, 293 K, oxygen bubbling.

It was found that the rate constant k_{2b} is sensitive to the oxygen concentration in the reaction system. Similar kinetic pattern is observed when the reaction is carried out with continuous argon bubbling: complete nitrosobenzene consumption in the course of deoxygenation, the pseudo-first-order reaction kinetics under the conditions of a phosphine excess over **1a**, and retention of the overall second order (the first order with respect to both reactants). The apparent rate constant k_{2b} determined under an argon atmosphere increases by approximately two times (by four times for **2c**) (see Table 1). Moreover, it was assumed that oxygen present in technical argon can affect the value of k_{2b} . We specially purified argon from oxygen and found for phosphines **2a** and **2d** that in "pure" argon the rate constant k_{2b} increases additionally by 10–20% (see Table 1).

The explanation of the influence of oxygen on the kinetics of the reaction of ArNO with phosphines is worth of more detailed investigation. Now we will advance hypotheses that explain the observed regularities. As already mentioned above, the partial regeneration of nitrosobenzene according to Scheme 6 (reaction (5)) was concluded²³ on the basis of the reaction product analysis.

Scheme 6



α is the content of the *trans*-isomer of formed nitroso oxide.

The *cis*-isomer of ArNOO undergoes intramolecular isomerization (see Scheme 2, thermal route), and the mechanism of this reaction was studied earlier.^{20,21,44–46}

We do not reject the possibility of this mechanism for ArNO regeneration and note an alternative possibility for the observed effect manifestation. Under an oxygen atmosphere nitrenes are efficiently replaced by the corresponding nitroso oxides (see Scheme 6, reaction (4)). However, the reaction of nitrene with the nitroso compound to form an azoxy product is known under the conditions of oxygen deficiency (see Scheme 6, reaction (6)). For the complete interception of nitrene, the stoichiometry of consumption of ArNO and R₃P should tend to the ratio 2 : 1, which approximately corresponds to the scale of increasing the rate constant k_{2b} in argon compared to that in oxygen. It is most likely that the presence of O₂ in the system decreases the probability of reaction (6) and, as a consequence, the value of rate constant k_{2b} . At the moment it is difficult to conclude which explanation is more probable. However, the combined action of both factors cannot be excluded. From the practical viewpoint, the rate constant k_{2b} measured in an aerated medium seems interesting, because nitroso oxides are generated just in these conditions.

The activation parameters of the rate constants of reaction (2b) were determined for all studied phosphines, except **2b** (see Table 2). As in the reaction involving triphenyl phosphite, the observed low values of pre-exponential factors indicate substantial losses of the entropy in the transition state. A strong decrease (by 16 kJ mol⁻¹) in the activation energy was observed upon the introduction of the methyl substituent with usually weak electronic effects into the aromatic ring of phosphine. The introduction of the fluorine atom into the aromatic ring, on the contrary, decreases the reactivity and somewhat increases the activation energy.

Chemiluminescence study of the kinetics of the reaction of nitrosobenzenes with phosphines. Chemiluminescence was recently found²⁵ in the deoxygenation of nitroso compounds by triphenylphosphine, and its intensity maximum is observed in the visible spectral range at ~570 nm. The scheme of the process performed earlier²⁵ is similar to Scheme 6. The emitter of the CL found in the reaction with triphenylphosphine is triphenylphosphine imine formed by the interaction of triphenylphosphine and triplet nitrene (Scheme 7).

Scheme 7



The kinetic analysis of the process indicates that the CL decay rate is limited by the rate of interaction for the reactants.²⁵ This makes it possible to use the CL method

for kinetic measurements of the reactions between triphenylphosphine derivatives and nitrobenzene in which the photoreaction is a kinetic indicator for the rate-determining step of the process. The reaction rate was monitored under the conditions of a considerable phosphine excess over PhNO. The CL intensity decay rigidly corresponded to an exponential law. All measurements in the temperature range 293–323 K were carried out at least three times. The reaction rate constants k_{2b} are given in Table 1. The results of calculation for the activation parameters of the reaction are presented in Table 2. The high reproducibility of the results obtained by two methods (KSP and CL) confirms correctness of the kinetic analysis for the CL scheme. In addition, the CL method made it possible to study the temperature dependence of the reaction rate constant for highly reactive *para*-methoxysubstituted phosphine.

Electronic effects in the reaction of nitrobenzenes with phosphines. The presented results show that a strong influence of substituents on the reactivity is manifested in the studied reaction. To take an additional information, we studied the kinetics of reaction (2b) involving *para*-methoxysubstituted nitrosobenzene **1b**. The kinetics of the reaction of **1b** with phosphines **2a–d** was studied using the above described procedure at the absorption maximum of **1b** (730 nm). The results of determination of the rate constant k_{2b} are presented in Table 1. The kinetic studies were carried out under oxygen at room temperature, and the initial concentration of **1b** was, as a rule, $3 \cdot 10^{-4}$ mol L⁻¹. A comparison of the experimental results for PhNO and 4-MeOC₆H₄NO shows that the introduction of the electron-donor substituent MeO into the aromatic ring of the nitroso compound sharply decreases the reactivity of the latter. The scale of the effect of H atom replacement by the methoxy group in nitrobenzene is two orders of magnitude. This surprisingly strong influence of the structure of ArNO on their reactivity in the reaction with phosphines provides possibilities to control the nitroso oxide generation rate by choosing ArNO, which is another advantage of the proposed method for the chemistry of nitro oxides.

Finally, our results make it possible to evaluate the influence of the phosphine structure on the reactivity in the framework of the widely used Hammett correlations. To estimate the electronic substituent effects, the Hammett constants σ (see Ref. 47), which describe the total effect of substituent including the inductive and resonance components, were used for the substituents. Obviously, the steric effect of the studied reaction is insubstantial. In three reaction series (the reactions of PhNO with phosphines under either O₂ or Ar and of 4-MeOC₆H₄NO with phosphines in the presence of oxygen), the following correlation was studied:

$$\log k_{2b} = \log k_{2b}^0 + \rho\sigma, \quad (\text{III})$$

where ρ is the constant of the reaction series reflecting the scale of the substituent effect on the rate constant, and σ is the substituent constant in the Hammett scale.

In all cases, the angular coefficient is negative; *i.e.*, in all reaction series, reaction (2b) is accelerated by the electron-donor substituents in a phosphine molecule. This result and the above mentioned decrease in the reactivity of 4-MeOC₆H₄NO compared to that of PhNO indicate that the nitroso compounds manifest the electrophilic properties in the studied reaction. The angular coefficient of the Hammett dependence has the following values: $\rho = -2.7 \pm 0.3$ (correlation coefficient $r = 0.99$) for the reaction of nitrosobenzene with argon bubbling into the reaction system, $\rho = -2.3 \pm 0.8$ ($r = 0.90$) in the reaction of nitrosobenzene in the presence of oxygen, and $\rho = -3.4 \pm 0.6$ ($r = 0.97$) for the reaction of *para*-methoxynitrosobenzene under an O₂ atmosphere.

Calculation of the reaction mechanism by the DFT method.

The activation parameters of the reaction of nitrosobenzene with triarylphosphines are linearly interrelated (see Table 2); *i.e.*, the studied reaction exhibits the compensation effect

$$\log A = (1.56 \pm 0.07) + (0.142 \pm 0.003)E_a,$$

$$r = 0.9995.$$

The compensation dependence of the activation energy on the pre-exponential factor indicates the general reaction mechanism for all phosphines. In addition, the low value of $\log A$ (the "normal" value for the bimolecular reaction is ~ 10 – 11) indicates a substantial entropy loss in the transition state of the studied reaction. The authors²⁴ suggest for the related reaction of 2-nitrosobiphenyl with triethyl phosphite that the low value of $\log A$ and, correspondingly, the high negative value of the activation of

entropy are explained by the formation of the transition state with charge separation and a loss of degrees of freedom. It is assumed that an intermediate of the ArN[−]—O—P⁺R₃ type is formed in the transition state and then decomposes to the reaction products. It is likely that this assumption can be extended to the reaction of nitrosobenzenes with phosphines.

In connection with the above, the DFT theoretical simulation of the studied reactions was performed. A series of different functionals (M06L, TPSSSTPSS, M06, TPSSh, B3LYP, CAM-B3LYP, LC-wPBE) was tested in combination with the Pople split-valence triple polarized basis set 6-311+G(d,p). The equilibrium structures of all reactants were calculated and the transition states (TS) of all studied transformations were localized using the indicated approximations. The TS of the reaction of **1a** with **2d** and triphenyl phosphite determined by the M06L/6-311+G(d,p) method are exemplified in Fig. 3. A strong effect of the density functional nature on the calculated value of the activation barrier was revealed in the course of simulation. For example, for reaction **1a** + **2a** (ignoring solvation effects), the enthalpy of activation (ΔH^\ddagger) increases from 39.4 (M06L) to 112.7 (LC-wPBE) kJ mol^{−1} in the order of functionals presented above. It can be assumed that the multiconfigurational character of the wave function for the TS is a reason for the observed non-reproducibility of the values of ΔH^\ddagger , since singlet nitrene is one of the reaction products. The static component of electron correlation plays a substantial role in these systems and is ignored in the framework of one-determinant description of the wave function. The observed scatter of ΔH^\ddagger values shows the ability of different density functionals to describe similar states more or less adequately.⁴⁸

In spite of considerable differences in estimation of the activation barrier for the reaction of nitrosobenzenes with

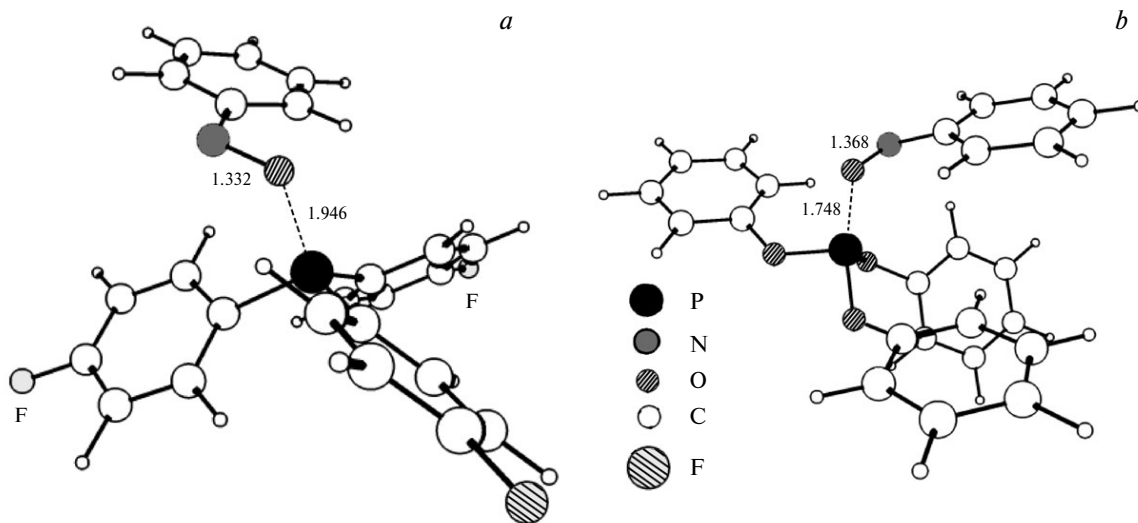


Fig. 3. Transition states of the reactions of nitrosobenzene (**1a**) with (4-FC₆H₄)₃P (**2d**) (a) and triphenyl phosphite (b) localized in the M06L/6-311+G(d,p) approximation. Interatomic distances are given in Å.

Table 3. Chemical potentials of the reagents and properties of the transition state of the reactions of nitrosobenzene with organic phosphorus(III) compounds

Reaction	μ/au		Properties of transition state of reaction				Properties of BCP P \cdots O		
	PhNO	R ₃ P	$\nu_{\text{imag}}/\text{cm}^{-1}$	$r(\text{N}\cdots\text{O})$ Å	$r(\text{P}\cdots\text{O})$ Å	$\Delta Q_{\text{PCM}}/\text{au}$	ρ	L	$ \lambda_1/\lambda_3 $
							au		
PhNO + 2b	0.162	0.112	272i	1.329	1.979	0.383	0.104	0.014	0.503
PhNO + 2c	0.162	0.116	277i	1.328	1.970	0.362	0.105	0.009	0.514
PhNO + 2a	0.162	0.125	294i	1.331	1.952	0.330	0.108	0.009	0.514
PhNO + 2d	0.162	0.136	287i	1.332	1.946	0.323	0.110	-0.009	0.549
4-MeOC ₆ H ₄ NO + 2a	0.149	0.125	292i	1.341	1.906	0.216	0.116	-0.046	0.636
PhNO + (PhO) ₃ P	0.162	0.131	292i	1.368	1.748	0.327	0.149	-0.030	0.615

Notes. Accepted designations: μ is the chemical potential of reagents; $\mu = -(\epsilon_{\text{HOMO}} + \epsilon_{\text{LUMO}})/2$, where ϵ are the energies of the HOMO and LUMO, respectively; BCP P \cdots O is the bond critical point according to the results of AIM analysis of the electron density; ν_{imag} is the only one imaginary frequency in the calculated vibrational spectrum verifying the transition state; r are intermolecular spacings; ΔQ_{PCM} is the excessive electron density on nitrosobenzene in the transition state (Mulliken analysis with allowance for the polarization of the TS by the solvent (MeCN) in the framework of the IEFPCM model); ρ is the electron density; L is the electron density Laplacian, $L = \nabla^2\rho$; λ_1 and λ_3 are eigenvalues of the electron density Hessian.

R₃P, all functionals used correctly reproduce the relative reactivity in a series of phosphines **2a–d** and a substantial increase in the activation energy of the reaction **1b** + **2a** and in the reaction of PhNO with (PhO)₃P which corresponds to the experimental data (see Table 2). Solvation that was taken into account in the framework of the IEFPCM polarizable continuum is an important stabilization factor. The results of DFT calculations obtained by the most adequate for the system functional (M06L) are given in Tables 2 and 3.

An analysis of the geometric structure and the electron distribution in the TS of the studied reactions showed, first, their high correspondence to the experimental data and, second, complete consistency of the hypothesis proposed²⁴ for the reaction mechanism.

We revealed a series of the regularities.

(1) The change in the P \cdots O interatomic distance in the TS and the value of activation barrier are antipate: the maximum length of the formed bond (1.979 Å) is observed in the TS of the reaction of PhNO with the most reactive phosphine **2b**, whereas in the TS of the reaction of nitrosobenzene with triphenyl phosphite $r(\text{P}\cdots\text{O})$ is much shorter (1.748 Å).

(2) An excessive electron density is accumulated on the nitroso compound in the transition state, and the degree of electron density transfer correlates with the electronic properties for the *para*-substituent in a series of phosphines **2a–d**. The Mulliken analysis (with allowance of the polarization of the TS by the solvent) gives a change in the excessive electron density from 0.323 au for **2d** to 0.383 au for **2c** (see Table 3). In this series, the tendency is more important that the absolute value because reliability of the Mulliken analysis is often low especially when diffuse functions in the basis set are used.⁴⁸ A significant charge transfer from R₃P to ArNO is confirmed by the

results of NBO and AIM analyses of the wave function, according to which 0.7–0.8 au of the negative charge is localized on the nitroso compound.

(3) As mentioned above, the incipient P \cdots O bond is the most remarkable geometric characteristic of the studied reaction. The AIM analysis of the TS wave function made it possible to characterize the properties of the bond critical point (BCP) for this pair of atoms (see Table 3). Note a comparatively low electron density ρ in the BCP and the minimum value of ρ in a series of studied TS is observed for the reaction of PhNO with **2b**, *i.e.*, for the reaction that proceeds with the lowest activation barrier and, *vice versa*, the maximum value of ρ is observed for the TS of the reaction PhNO + (PhO)₃P.

(4) According to the published work,⁴⁹ the type of chemical bond can be characterized by such BCP parameters as the ratio of minimum and maximum eigenvalues of the Hessian ρ taken by modulus $|\lambda_1/\lambda_3|$ and the electron density Laplacian $L[\rho]$. The data in Table 3 show that $|\lambda_1/\lambda_3| < 1$ and L is low in all cases. This interactions of atoms is named "closed-shell interaction" and is characteristic of ionic and strongly polar covalent bonds, since the withdrawal of electron density from the BCP towards nuclei predominates, and its measure is λ_3 .⁴⁹ For the same reason, the electron density in the BCP is fairly low (see above).

Thus, the results of DFT simulation of the reaction of ArNO with R₃P are well consistent with the kinetic data, explain the differences observed in the reactivity of the reactants, and theoretically confirm Cadogan's hypothesis^{22,24} that the reaction proceeds through the TS with a high degree of charge separation on the reaction center. This results in substantial losses of the activation entropy (see Table 2). In addition, the high polarity of the TS assumes its efficient solvation. Perhaps, peculiarities of

specific solvation of the TS, which were ignored in the framework of our theoretical model, result in the appearance of a compensation effect in a series of *para*-substituted phosphates.

Thus, the kinetics of the reactions of nitrosobenzenes with trivalent phosphorus compounds was studied by two independent methods: kinetic spectrophotometry and chemiluminescence. The obtained data create a theoretical basis for a substantiated choice of conditions for the dark (*i.e.*, non-photolytic) generation of aromatic nitroso oxides. The revealed strong dependence of the rate constant on the structures of the reactants makes it possible to generate ArNOO in a wide range of rates, which can be useful for choosing optimum experimental conditions to study the chemical properties of nitroso oxides.

This work was financially supported by the Division of Chemistry and Materials Science of the Russian Academy of Sciences (Program "Intermediates of Chemical Reactions, Their Direct Detection and Stabilization, and Determination of Structural Parameters") and the Russian Foundation for Basic Research (Project No. 13-03-00201).

References

1. E. M. Chainikova, S. L. Khursan, R. L. Safiullin, *Dokl. Phys. Chem. (Engl. Transl.)*, 2003, **390**, 163 [*Dokl. Akad. Nauk*, 2003, **390**, 796].
2. R. L. Safiullin, S. L. Khursan, E. M. Chainikova, V. T. Danilov, *Kinet. Catal. (Engl. Transl.)*, 2004, **45**, 640 [*Kinet. Katal.*, 2004, **45**, 680].
3. E. M. Chainikova, S. L. Khursan, R. L. Safiullin, *Kinet. Catal. (Engl. Transl.)*, 2004, **45**, 794 [*Kinet. Katal.*, 2004, **45**, 842].
4. E. M. Chainikova, S. L. Khursan, R. L. Safiullin, [*Kinet. Catal. (Engl. Transl.)*, 2006, **47**, 549 [*Kinet. Katal.*, 2006, **47**, 566].
5. M. R. Talipov, A. B. Ryzhkov, S. L. Khursan, R. L. Safiullin, *J. Struct. Chem. (Engl. Transl.)*, 2006, **47**, 1051 [*Zh. Strukt. Khim.*, 2006, **47**, 1062].
6. E. M. Chainikova, R. L. Safiullin, *Kinet. Catal. (Engl. Transl.)*, 2009, **50**, 527 [*Kinet. Katal.*, 2009, **50**, 551].
7. V. S. Khursan, E. M. Chainikova, R. L. Safiullin, *High Energy Chem. (Engl. Transl.)*, 2009, **43**, 467 [*Khim. Vys. Energ.*, 2009, **43**, 523].
8. E. M. Chainikova, R. L. Safiullin, *Russ. Chem. Bull. (Int. Ed.)*, 2009, **58**, 2437 [*Izv. Akad. Nauk, Ser. Khim.*, 2009, 2359].
9. M. R. Talipov, S. L. Khursan, R. L. Safiullin, *J. Phys. Chem. A*, 2009, **113**, 6468.
10. V. S. Khursan, O. A. Kovaleva, E. M. Chainikova, M. R. Talipov, R. L. Safiullin, *High Energy Chem. (Engl. Transl.)*, 2010, **44**, 284 [*Khim. Vys. Energ.*, 2010, **44**, 313].
11. M. R. Talipov, S. L. Khursan, R. L. Safiullin, [*Russ. J. Phys. Chem. A (Engl. Transl.)*, 2011, **85**, 364 [*Zh. Fiz. Khim.*, 2011, **85**, 427].
12. Y. Sawaki, S. Ishikawa, H. Iwamura, *J. Am. Chem. Soc.*, 1987, **109**, 584.
13. E. A. Pritchina, N. P. Gritsan, *J. Photochem. Photobiol. A*, 1988, **43**, 165.
14. N. P. Gritsan, E. A. Pritchina, *J. Inform. Rec. Mater.*, 1989, **17**, 391.
15. S. Ishikawa, S. Tsuji, Y. Sawaki, *J. Am. Chem. Soc.*, 1991, **113**, 4282.
16. S. Ishikawa, T. Nojima, Y. Sawaki, *J. Chem. Soc., Perkin Trans. 2*, 1996, 127.
17. T. Harder, P. Wessig, J. Bendig, R. Stösser, *J. Am. Chem. Soc.*, 1999, **121**, 6580.
18. H. Inui, M. Irisawa, S. Oishi, *Chem. Lett.*, 2005, **34**, 478.
19. E. A. Pritchina, N. P. Gritsan, T. Bally, *Phys. Chem. Chem. Phys.*, 2006, **8**, 719.
20. E. M. Chainikova, R. L. Safiullin, A. N. Teregulova, L. V. Spirikhin, E. G. Galkin, *Dokl. Chem. (Engl. Transl.)*, 2012, **442**, 30 [*Dokl. Akad. Nauk*, 2012, **442**, 493].
21. E. Chainikova, R. Safiullin, L. Spirikhin, A. Erastov, *Tetrahedron Lett.*, 2013, **54**, 2140.
22. J. I. G. Cadogan, *Q. Rev., Chem. Soc.*, 1968, **22**, 222.
23. E. M. Chainikova, R. L. Safiullin, *Russ. Chem. Bull. (Int. Ed.)*, 2009, **58**, 926 [*Izv. Akad. Nauk, Ser. Khim.*, 2009, 906].
24. J. I. G. Cadogan, A. Cooper, *J. Chem. Soc. B*, 1969, 883.
25. V. A. Shamukaev, A. N. Teregulova, S. S. Ostakhov, R. L. Safiullin, *High Energy Chem. (Engl. Transl.)*, 2013, **47** [*Khim. Vys. Energ.*, 2013, **47**, 66].
26. G. H. Coleman, Ch. M. McCloskey, F. A. Stuart, *Org. Synth.*, 1955, Coll. Vol. **3**, 668.
27. I. Guben, *Metody organicheskoi khimii [Methods of Organic Chemistry]*, Goskhimizdat, Moscow—Leningrad, 1949 (in Russian).
28. V. M. Plets, *Organicheskie soedineniya fosfora [Organic Phosphorus Compounds]*, Oborongiz, Moscow, 1940 (in Russian).
29. M. J. Frisch, G. W. Trucks, H. B. Schlegel, G. E. Scuseria, M. A. Robb, J. R. Cheeseman, G. Scalmani, V. Barone, B. Mennucci, G. A. Petersson, H. Nakatsuji, M. Caricato, X. Li, H. P. Hratchian, A. F. Izmaylov, J. Bloino, G. Zheng, J. L. Sonnenberg, M. Hada, M. Ehara, K. Toyota, R. Fukuda, Y. Hasegawa, M. Ishida, T. Nakajima, Y. Honda, O. Kitao, H. Nakai, T. Vreven, J. Montgomery, Jr., J. E. Peralta, F. Ogliaro, M. Bearpark, J. J. Heyd, E. Brothers, K. N. Kudin, V. N. Staroverov, R. Kobayashi, J. Normand, K. Raghavachari, A. Rendell, J. C. Burant, S. S. Iyengar, J. Tomasi, M. Cossi, N. Rega, J. M. Millam, M. Klene, J. E. Knox, J. B. Cross, V. Bakken, C. Adamo, J. Jaramillo, R. Gomperts, R. E. Stratmann, O. Yazyev, A. J. Austin, R. Cammi, C. Pomelli, J. W. Ochterski, R. L. Martin, K. Morokuma, V. G. Zakrzewski, G. A. Voth, P. Salvador, J. J. Dannenberg, S. Dapprich, A. D. Daniels, Ö. Farkas, J. B. Foresman, J. V. Ortiz, J. Cioslowski, D. J. Fox, *Gaussian-09, Rev. C1*, Gaussian, Inc., Wallingford (CT), 2009.
30. G. A. Zhurko, *ChemCraft, Version 1.6 (build 332)*; <http://www.chemcraftprog.com>.
31. A. D. Becke, *J. Chem. Phys.*, 1993, **98**, 5648.
32. C. Lee, W. Yang, R. G. Parr, *Phys. Rev. B*, 1988, **37**, 785.
33. T. Yanai, D. P. Tew, N. C. Handy, *Chem. Phys. Lett.*, 2004, **393**, 51.
34. J. Tao, J. P. Perdew, V. N. Staroverov, G. E. Scuseria, *Phys. Rev. Lett.*, 2003, **91**, 146401.
35. O. A. Vydrov, G. E. Scuseria, *J. Chem. Phys.*, 2006, **125**, 234109.
36. Y. Zhao, D. Truhlar, *Theor. Chem. Acc.*, 2008, **120**, 215.

37. Y. Zhao, D. G. Truhlar, *J. Chem. Phys.*, 2006, **125**, 194101.
38. A. D. McLean, G. S. Chandler, *J. Chem. Phys.*, 1980, **72**, 5639.
39. K. Raghavachari, J. S. Binkley, R. Seeger, J. A. Pople, *J. Chem. Phys.*, 1980, **72**, 650.
40. J. Tomasi, B. Mennucci, R. Cammi, *Chem. Rev.*, 2005, **105**, 2999.
41. A. E. Reed, L. A. Curtiss, F. Weinhold, *Chem. Rev.*, 1988, **88**, 899.
42. R. F. W. Bader, *Atoms in Molecules: A Quantum Theory*, Oxford Univ. Press, Oxford, 1994, 458 pp.
43. V. Talrose, A. N. Yermakov, A. A. Usov, A. A. Goncharova, A. N. Leskin, N. A. Messineva, N. V. Trusova, M. V. Efimkina, in *NIST Chemistry WebBook, NIST Standard Reference Database Number 69*, Eds P. J. Linstrom, W. G. Mallard, National Institute of Standards and Technology, Gaithersburg (MD), 2012, p. 20899.
44. M. R. Talipov, S. L. Khursan, R. L. Safiullin, *Russ. J. Phys. Chem. A (Engl. Transl.)*, 2012, **86**, 235 [*Zh. Fiz. Khim.*, 2012, **86**, 292].
45. E. M. Chainikova, R. L. Safiullin, L. V. Spirikhin, *Dokl. Chem. (Engl. Transl.)*, 2012, **442**, 12 [*Dokl. Akad. Nauk*, 2012, **442**, 200].
46. E. M. Chainikova, R. L. Safiullin, L. V. Spirikhin, M. F. Abdullin, *J. Phys. Chem. A*, 2012, **116**, 8142.
47. A. J. Gordon, R. A. Ford, *The Chemist's Companion: A Handbook of Practical Data, Techniques, and References*, Wiley, New York, 1972, 537 pp.
48. F. Jensen, *Introduction to Computational Chemistry*, John Wiley and Sons, Chichester, 2007.
49. I. S. Bushmarinov, K. A. Lyssenko, M. Yu. Antipin, *Russ. Chem. Rev.*, 2009, **78**, 283.

Received May 27, 2013